

# High-velocity optothermal whirlpool actuation at the air-water interface

R. Zibaei, M. G. Delli Santi, S. Castrignano and P. Malara\*

Consiglio Nazionale delle Ricerche, Istituto Nazionale di Ottica (INO), via Campi Flegrei 34, 80078 Pozzuoli, Naples, Italy.  email: pietro.malara@ino.cnr.it

*In a meniscus lifted above a free water surface by an optical fiber delivering near infrared radiation, the upper confinement of the heated buoyant liquid amplifies the surface temperature gradient, driving particularly strong thermocapillary effects. When the temperature gradient within the meniscus becomes very large, the stationary convection flow destabilizes in a periodic pattern of surface hydrothermal waves. We show that these light-fueled waves can be controlled to a large extent by acting on the system parameters, and harnessed to propel buoyant macroparticles along stable closed trajectories at exceptionally high speeds. With 20–30 mW of input power at 1550 nm, we observe fast linear oscillations of 0.1–1 mm particles with peak velocities up to 2 cm/s and a whirlpool-like stable orbital motion with rotation rate up to 600 rpm, the largest reported so far for optothermal actuation. These findings establish a new efficient method for contactless actuation on liquid surfaces with direct application in microfluidics and in the realization of efficient light-powered micromotors. At the same time, the proposed fiber-meniscus configuration provides a simple and adaptable platform for studying optothermal fluid instabilities and for generating and controlling surface thermocapillary waves.*

Thermocapillary effects, also known as Marangoni effects, arise from surface tension gradients generated by local temperature differences on the interface between fluids, and are known to create distinct transport phenomena from regions of low surface tension (high temperature) to regions of high surface tension (low temperature). For this reason these effects play a significant role in manipulating small-scale particles at fluid interfaces. At the air-water interface, even small deviations from the ambient temperature created with optical methods are sufficient to displace, rotate or move small particles along complex trajectories [1-6]. Indeed, among all contactless actuation techniques, thermocapillary effects on the water surface stand out for the large velocities achievable with small temperature gradients (up to a few mm/s), and are largely used to mediate the conversion of light into work, through laser-driven microswimmers or laser-heated particles with asymmetrical heat conductivity [8-12].

In this work, we investigate experimentally the thermocapillary convection in an optically heated axisymmetric water meniscus and harness its unique instability dynamics to actuate buoyant particles at extremely fast velocities on the liquid surface, demonstrating a new and efficient method to convert light into mechanical work.

Thermocapillary convection in liquids with an axially-symmetric heat source has been extensively studied, both theoretically and experimentally [13-20]. When the source of heat is close to the surface, a toroidal convection cell develops around the symmetry axis, characterized by a radial surface flow directed outwards and a sub-surface replenishment flow directed inwards. The flows are stationary and depend on the temperature gradient along the liquid surface, but for large T gradients they can destabilize, generating periodical hydrothermal waves.

In our experiments the axisymmetric meniscus is lifted from a free water surface by a cleaved optical fiber. Besides supporting the meniscus, the optical fiber also acts as a microscopic

heater and probe, allowing to induce temperature variations through infrared radiation and measure them through the water refractive index response. As the meniscus is lifted, hot water gets more and more confined, achieving a large temperature difference with the pool, that drives strong thermocapillary effects. After a critical height, an oscillatory convection regime is observed with large temperature fluctuations. In this regime, the balance between surface convection waves and meniscus capillary attraction can be controlled to actuate buoyant particles at high velocity along extremely stable trajectories.

## Results

**Experimental setup.** A single-mode optical fiber (125  $\mu\text{m}$  diameter) cleaved at right angle lifts an axisymmetric meniscus from a pool of Milli-Q water at ambient temperature, in a glass circular container 4 cm wide and 1 cm deep (fig 1a). The fiber delivers near infrared radiation (NIR) at 1.5  $\mu\text{m}$  wavelength from an amplified spontaneous emission source (ASE), and its distance  $h$  from the free water surface can be controlled by a micrometric translation stage. The radiation reflected by the immersed fiber end is collected through a 50% fiber splitter and sent to a photodetector to monitor the refractive of the water in the upper meniscus  $n_w$ . The reflectivity of the fiber-water interface is related to  $n_w$  by the Fresnel relation  $R = \left(\frac{n_f - n_w}{n_f + n_w}\right)^2$ , where  $n_f$  is the refractive index of the optical fiber. A 30f/s digital microscope placed upon or underneath the glass container is used to visualize the motion of particles on the liquid surface.

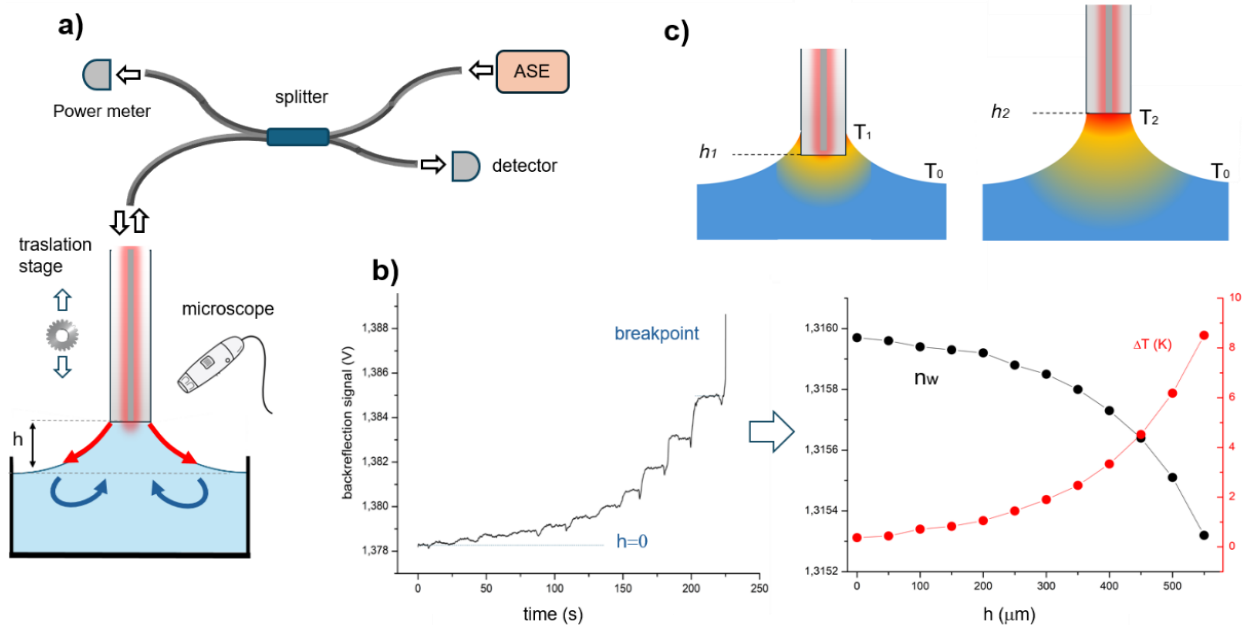


**Fig. 1: meniscus setup and enhancement of thermal gradient.** (a) Schematic of the experimental setup: a right-angle cleaved optical fiber is lifted vertically from a free water surface, creating an axisymmetric meniscus. The fiber delivers infrared radiation which heats the meniscus producing a toroidal convection cell, and at the same time measures the temperature of water at the fiber interface through the

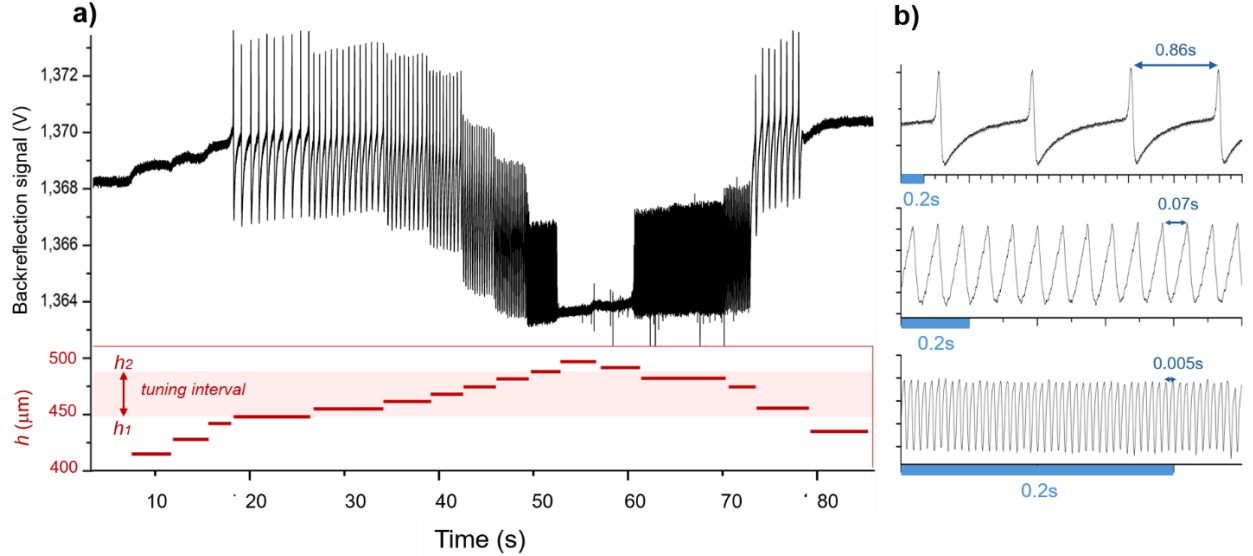
intensity reflected at the fiber water interface. (b) Reflection signal recorded while lifting the meniscus in 50-micron steps. The changes in the reflected light intensity as the meniscus height increases reflect variations in the water refractive index  $n_w$ , which in turn correlate with temperature variations  $\Delta T$  in the upper meniscus. (c) Conceptual illustration of the temperature gradient evolution in the meniscus: as the fiber is lifted, the less dense hot water is confined near the fiber, enhancing the surface temperature gradient.

The cleaved fiber, initially placed in contact with the free liquid surface ( $h=0$ ), is lifted vertically in 50- $\mu\text{m}$  steps, while recording the backreflection signal. As shown in Fig. 1b, the reflectivity of the fiber–water interface increases steadily at each lifting step until the meniscus breaks, following a trend that corresponds to a nonlinear decrease of  $n_w(h)$  (right plot, black dots). This RI reduction, already noted in [21], occurs only under near-infrared irradiation, indicating that it originates from the water temperature rise caused by radiation absorption. The variations of the meniscus equilibrium temperature at the various height steps are calculated from the measured  $n_w(h)$  as  $\Delta T = n_w / \frac{dn_w}{dT}$ , using the approximate value  $\frac{dn_w}{dT} = -0.8 * 10^{-4}$  [22] (Fig. 1b, red dots). The upper meniscus temperature shows a positive correlation with the backreflection signal and, over the whole lifting process, increases by  $7\pm1\text{K}$ . This trend can be intuitively explained by considering that hot water is pushed upwards toward the heat source by its buoyancy and laterally constrained by the meniscus walls. Such confinement limits the thermal exchange, so the equilibrium temperature in the upper meniscus increases (see the sketch in Fig. 1c). Crucially for our experiments, this extra heating localized at the top of a 0.1 mm meniscus generates a particularly strong temperature gradient along the liquid surface, sensibly amplifying the effects of thermocapillary convection.

**Convection instability in the time domain.** When the power of the heating NIR radiation is set above a critical value, a time-dependent instability manifests spontaneously. In Fig. 2a, we display an example of backreflection signal recorded with 20 mW NIR power while varying  $h$  as illustrated in the bottom panel. Fig. 2a well illustrates the rich instability dynamics in the meniscus:

- (0-25s): initially, the signal reproduces the same increasing-temperature pattern of Fig. 1, but passed a critical height  $h_1$  a pulsed instability onsets, with an amplitude corresponding to a  $\sim 5\text{K}$  temperature fluctuation and a periodicity around 1Hz. At this stage the average backreflection level remains constant, meaning that the average meniscus temperature does not change.
- (25-50s): for larger values of  $h$ , the oscillation frequency increases and the average backreflection level decreases, i.e. as opposed to the stationary situation, the meniscus now cools down during the lift-up process. At the same time, the oscillation transitions from a pulsed to a triangular waveform (see Fig. 2b).
- (50-90s): the lifting continues and reaches a second threshold  $h_2$ , where the oscillation stops completely. The heights values  $h_1$  and  $h_2$  define an interval where the trends for frequency, average temperature and instability waveform are completely reversible and therefore controllable to a large degree. Indeed, when  $h$  is reduced after reaching  $h_2$  (60-90s interval of

Fig.2a), the instability onsets again, reproducing the same patterns backwards and leading once more to a stationary signal when eventually  $h_1$  is crossed in the opposite direction.



**Controlling the meniscus thermocapillary instability.** (a) The upper panel displays the backreflection signal from the fiber-water interface (20 mW input power), which is correlated to the temperature at the meniscus apex. The bottom panel shows the corresponding vertical displacement of the optical fiber over time. A pulsed instability onsets around  $h \sim 440$   $\mu\text{m}$ . With increasing  $h$  values it evolves into a faster triangular waveform and then ceases completely when  $h \sim 470$   $\mu\text{m}$ .  $h_1$  and  $h_2$  define a region where the instability is reversible and can be precisely controlled. (b) Magnified view of the backreflection signal, highlighting the transition from a pulsed to a fast triangular waveform for different values of  $h$ .

The described temporal dynamics of the backreflection signal reflect an oscillatory convection scenario, where hydrothermal surface waves periodically push the heated water away from the meniscus, producing rapid temperature fluctuations. When the threshold  $h_1$  is crossed (fig.2a, around  $t=20$  s), a pulsed regime with  $\sim 1$  s periodicity onsets, without any variation in the average meniscus temperature. This means that all the hot water that was previously being displaced in  $\sim 1$  s by the stationary thermocapillary flow gets to be displaced instantaneously in a single pulse event. At this stage, the effect of thermocapillary pulses is so large that it can be observed on the microscope (see *video0*). As discussed in the following, this plays a crucial role in the actuation of particles on the liquid surface. For larger values of  $h$  the hydrothermal pulses become more frequent and eventually transition to a triangular oscillation. In this situation the time available for thermal build-up in the meniscus water decreases, resulting in a lower average temperature and smaller oscillations, i.e. a cooling  $\Delta T(h)$  trend, reversed with respect to the stationary-flow case. Eventually, the temperature oscillations become so rapid and small that only their average effect is detected, giving rise to the second threshold  $h_2$ .

**Actuation of particles by hydrothermal waves.** Additional insights in the meniscus instability can be gained from the motion of buoyant particles on the water surface that are subject to the hydrodynamic drag of the convection waves. In these experiments, we used polypropylene (p.p) and acrylic urethane (a.u.) fragments ranging from 10 to 500 microns as tracers, although in some cases also unidentified particles captured on the water surface proved useful to visualize the effect of thermocapillary waves. Besides the hydrodynamic drag force  $F_H$ , buoyant particles also experience a meniscus attraction force  $F_C$ : this ubiquitous phenomenon is colloquially known as the “Cheerios effect” [23] and stems from the capillary interactions of nearby menisci.

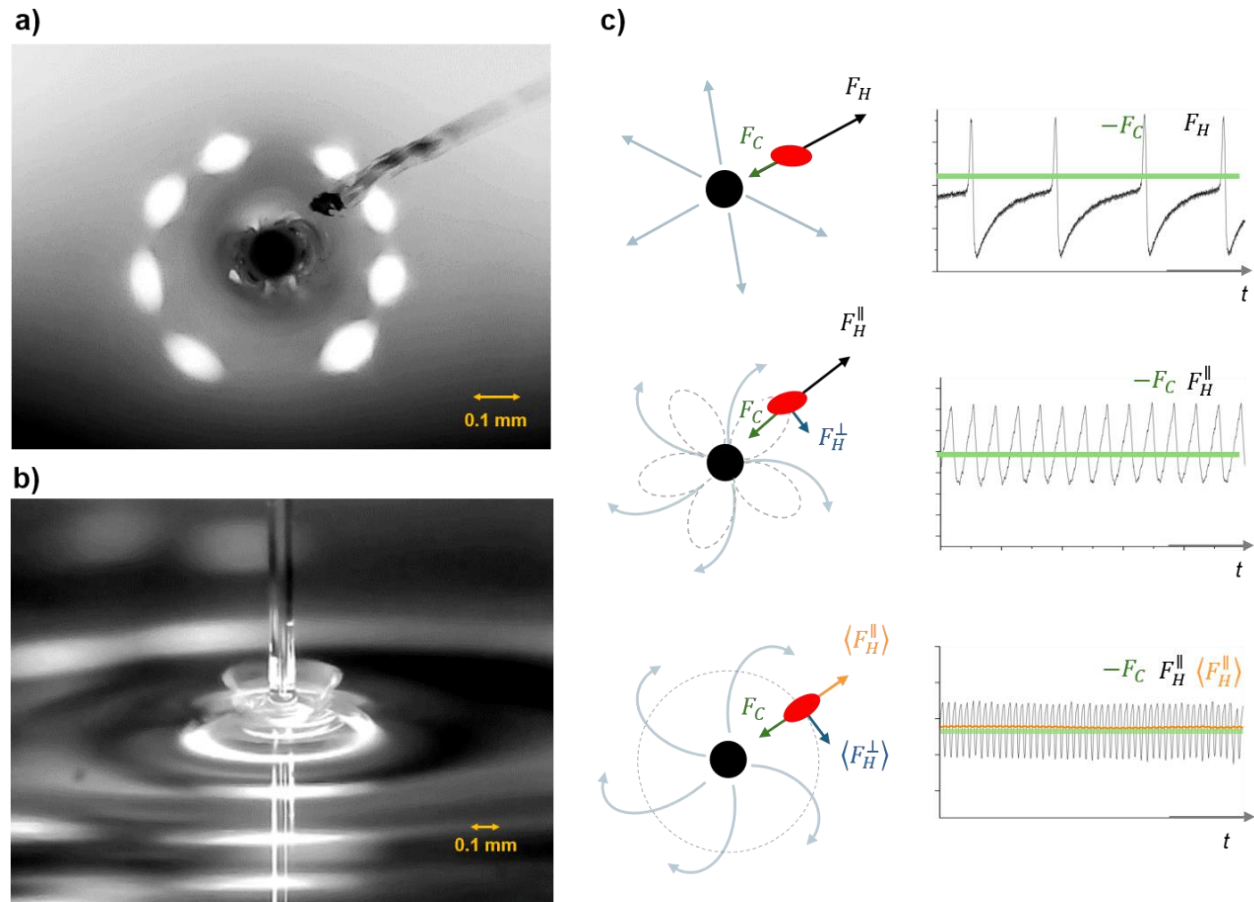


**Fig 3: Actuation of buoyant particles by hydrothermal waves and capillary attraction.** (a) Radial oscillation: superposition of frames from video1, additional examples in video2,3;4. In the view from below: the white spots around the fiber are the reflections of the microscope lights on the water surface. (b) whirlpool orbital motion (superposition of frames from video5, additional examples in video6,7,8), top view. (c) space and time domain force diagrams show how different actuation patterns arise by increasing the thermal gradient, because of the concomitant frequency increase and spiralization of the hydrothermal waves. The maximum velocity achieved is 2cm/s for the oscillatory motions (measured from video2) and 600 rpm for the orbital motion (measured from video8).

In stationary-flow conditions, the dominant force for a given particle shape and size determines whether the particle is drawn toward the meniscus or pushed away from it. However, once instability sets in, the balance between  $F_H$  and  $F_C$  can change dynamically, producing various periodic motions.

In the initial stages of the instability *radial oscillations* are observed: a typical particle trajectory is illustrated in Fig.3a with a superposition of frames from *video1* (a.u. fragment). As shown in the force diagram of Fig.3c (upper panel), at this stage the meniscus convection is governed by strong pulses with a radial velocity field, whose drag force  $F_H$  can temporarily prevail on the steady meniscus attraction and shoot particles outwards with a velocity as high as 2cm/s. In the time between pulses the force balance reverses again in favour of  $F_C$  and particles are drawn back towards the meniscus. Examples of oscillatory motions associated to this dynamics can be found in *video1* and *video2* (*p.p. and a.u. fragments, bottom view*). By tuning  $h$ , i.e. controlling the periodicity of hydrothermal waves, very fast and stable oscillations can be obtained (*video3, small p.p. particle, top view*).

When the fiber is further lifted, oscillatory radial motions evolve into petal-like trajectories (*video4, unidentified particle, top view*), reflecting the emergence of an azimuthal velocity component of the hydrothermal waves. The breakup of the radial velocity field of hydrothermal waves into an azimuthal spiral pattern is widely documented in fluids with large temperature gradients and axisymmetric heating geometries, like vertical rods [14,15], immersed wires [16] or differentially-heated liquid bridges [17-20]. In our setup, when the fiber is lifted, a similar distortion emerges alongside with the increasing oscillation frequency, causing  $F_H$  to break into a radial ( $F_H^{\parallel}$ ) and an azimuthal component ( $F_H^{\perp}$ ), as shown in see fig3c, mid panel.

If the frequency of hydrothermal waves becomes very large, it may happen that a particle can't follow instantaneously the rapid variations of  $F_H$  and only experiences a steady average drag force  $\langle F_H \rangle$ . In this situation, sketched in the lower panel of fig.3c,  $F_C$  and  $\langle F_H^{\parallel} \rangle$  do not produce radial oscillations, but balance the particle at an equilibrium distance from the meniscus, while  $\langle F_H^{\perp} \rangle$  drives it in a circular trajectory with locked orientation which resembles the motion of a particle caught in a whirlpool. An example of whirlpool-like motion is shown in fig.3b (frames superposition from *video5*) and in videos 5,6,7 (*video5: p.p. fragment, video6:a.u. fragment; video7: large a.u. raft*). The orbital velocity depends on specific geometry of the actuated body, but again it can be tuned by controlling the driving instability. This is clearly shown in *video8*, where, by tuning radiation power and meniscus height, the whirlpool rotation of an unidentified particle captured on the water surface is progressively increased up to 600 rpm, to our knowledge the largest angular velocity achieved with optothermal actuation. Larger particles (0.1-1 mm), integrate more effectively the fast  $F_H$  oscillations and are more prone to move directly in whirlpool mode. However, with intermediate-size particles (100-200 microns), which can follow the oscillations up to a critical frequency, it is possible to arbitrarily switch from oscillatory to whirlpool motions only by increasing  $h$ , as shown in *video9* and *video10*.

As a final remark, we note that all the described effects are stronger in freshly-filtered water, and harder to observe or totally inhibited when water has been exposed to air for a

prolonged time. This phenomenon, also reported in [4], is associated to the formation of a thin adsorption layer on the water surface which influences the stability and the structure of the convection flow induced by heat [24].

## Conclusions

In an axisymmetric water meniscus irradiated from above, natural buoyancy confines the heat and sensibly enhances the surface thermal gradient, leading to strong thermocapillary convection instability effects. In the unstable convection regime, by acting on the meniscus height and laser power, the surface hydrothermal flow can be arbitrarily shaped in pulses or fast oscillations and its velocity field can be as well tuned from a radial to a spiral pattern. The ability of precisely controlling the oscillatory surface flows can be exploited to actuate buoyant particles on the water surface. Indeed, by balancing the hydrodynamic drag of the surface waves and the meniscus capillary attraction, particles in the meniscus vicinity can be driven in stable oscillations or locked orbital trajectories. Compared to other pseudo-orbital and oscillatory motions observed with heated optically-trapped microparticles or in evaporating droplets [4-6], the actuation obtained with the meniscus geometry is largely more stable, controllable, and can reach velocities in the order of a few cm/s. These features while envisioning a direct application in microfluidic manipulation and in the design of efficient light-powered micromotors, establish this setup as a versatile and accessible experimental platform for the fundamental study of hydrothermal waves in liquids.

## Data availability

Raw data that support the results of this study are available from the corresponding author upon reasonable request.

## References

1. Terrazas, R. et al. Thermocapillary micromanipulation: force characterization and Cheerios interactions. *J Micro-Bio Robot* **15**, 13–22 (2019).
2. Quispe, J., Muñoz, E. & Vela, E. Exploiting the transient behavior of thermocapillary convection flows to enhance non-contact mesoscale manipulation. *Appl. Phys. Lett.* **109**, 124102 (2016).
3. R. T. Mallea, A. Bolopion, J. -C. Beugnot, P. Lambert and M. Gauthier, "Laser-Induced Thermocapillary Convective Flows: A New Approach for Noncontact Actuation at Microscale at the Fluid/Gas Interface," in *IEEE/ASME Transactions on Mechatronics*, vol. 22, no. 2, pp. 693-704, doi: 10.1109/TMECH.2016.2639821.
4. Girot, A. et al. Motion of Optically Heated Spheres at the Water–Air Interface. *Langmuir* **32**, 2687–2697 (2016).
5. Zhong, M.-C., Wang, Z.-Q. & Li, Y.-M. Oscillations of absorbing particles at the water-air interface induced by laser tweezers. *Opt. Express, OE* **25**, 2481–2488 (2017).
6. K. Gupta; Kiran M. Kolwankar; B. Gore, J.A. Dharmadhikari; A. K. Dharmadhikari. Laser-driven Marangoni flow and vortex formation in a liquid droplet, *Physics of Fluids* 32, 121701 (2020)
7. Terrazas Mallea, R., Bolopion, A. Beugnot, J.C., Lambert, P. and Gauthier, M., in Intelligent Robots and Systems (IROS) (2017), pp. 408–413
8. Okawa, D., Pastine, S. J., Zettl, A. & Fréchet, J. M. J. Surface Tension Mediated Conversion of Light to Work. *J. Am. Chem. Soc.* **131**, 5396–5398 (2009).
9. Frumkin, V. Dipolar thermocapillary motor and swimmer. *Phys. Rev. Fluids* **4**, (2019).

10. Maggi, C., Saglimbeni, F., Dipalo, M., De Angelis, F. & Di Leonardo, R. Micromotors with asymmetric shape that efficiently convert light into work by thermocapillary effects. *Nat Commun* **6**, 7855 (2015).
11. Li, J. *et al.* Opto-Thermocapillary Nanomotors on Solid Substrates. *ACS Nano* **16**, 8820–8826 (2022).
12. Máthé, M. T. Ferroelectric nematic liquid crystal thermomotor. *Phys. Rev. E* **105**, (2022).
13. Mizev, A. I. Experimental Investigation of Thermocapillary Convection Induced by a Local Temperature Inhomogeneity near the Liquid Surface. 1. Solid Source of Heat. *Journal of Applied Mechanics and Technical Physics* **45**, 486–497 (2004).
14. Favre, E., Blumenfeld, L. & Daviaud, F. Instabilities of a liquid layer locally heated on its free surface. *Physics of Fluids* **9**, 1473–1475 (1997).
15. Wu, D., Tang, W., Wang, J. *et al.* On Chinese space station: pioneering space experiments unraveling the hydrodynamic instability of annular thermocapillary convection. *Sci Rep* **15**, 40886 (2025).
16. Kamotani, Y., Lee, J. H., Ostrach, S. & Pline, A. “An experimental study of oscillatory thermocapillary convection in cylindrical containers”. *Physics of Fluids A: Fluid Dynamics* **4**, 955–962 (1992).
17. Hoyas, S., Mancho, A. M., Herrero, H., Garnier, N. & Chiffaudel, A. “Bénard–Marangoni convection in a differentially heated cylindrical cavity”. *Physics of Fluids* **17**, 054104 (2005).
18. Arafune, K., Kinoshita, A., Fujiwara, Y. & Hirata, A. “Characterization of oscillatory Marangoni convection in liquid bridges
19. Rednikov, A. Ye., Colinet, P., Velarde, M. G. & Legros, J. C. “Rayleigh–Marangoni oscillatory instability in a horizontal liquid layer heated from above: coupling and mode mixing of internal and surface dilatational waves”. *J. Fluid Mech.* **405**, 57–77 (2000).
20. Frank, S. & Schwabe, D. Temporal and spatial elements of thermocapillary convection in floating zones. *Experiments in Fluids* **23**, 234–251 (1997).
21. P. Malara, A. Crescitelli, V. Di Meo, A. Giorgini, S. Avino, E. Esposito, A. Ricciardi, A. Cusano, I. Rendina, P. De Natale, G. Gagliardi, Resonant enhancement of plasmonic nanostructured fiber optic sensors, Sensors and Actuators B: Chemical, Volume 273,2018,Pages 1587-1592,ISSN 0925-4005,https://doi.org/10.1016/j.snb.2018.07.030.
22. Daimon, M. & Masumura, A. Measurement of the refractive index of distilled water from the near-infrared region to the ultraviolet region. *Appl Opt* **46**, 3811–3820 (2007).
23. D.Vella and L. Mahadevan, "The 'Cheerios effect'", Am. J. Phys., Vol. 73, No. 9, 2005
24. Mizev, A. Influence of an adsorption layer on the structure and stability of surface tension driven flows. *Physics of Fluids* **17**, (2005).

## Acknowledgements

This research was supported by the Italian Ministry of University and Research (MUR) within the PRIN 2022 program (Call for proposal D.D. n. 104 of 02/02/2022) – Project 2022YZEXBL\_PE2\_PRIN2022: *ID-SWAP: “interferometric detection of stretched water’s properties and their role in biological systems”* CUP: B53D23005340006

## Author contributions

Concept: PM; experiments: RZ, MGdS, PM; analysis and interpretation: PM, SC. All authors contributed to the manuscript.

## Competing interests

The authors declare no competing interests.